Deriving C_4 photosynthesis parameters by fitting intensive A/C_i curves

Haoran Zhou[1], Erol Akçay[1] and Brent R. Helliker[1]

[1] Department of Biology, University of Pennsylvania, Philadelphia, PA 19104, USA

Correspondence: Haoran Zhou

Address: 433 S University Ave.

314 Leidy Labs

Philadelphia, PA 19104

Phone: 1-215-808-7042

Email: haoranzh@sas.upenn.edu

Brent R. Helliker*: helliker@sas.upenn.edu*

Erol Akçay: *eakcay@sas.upenn.edu*

Running head*:* Deriving C_4 photosynthesis parameters

ABSTRACT

Measurements of photosynthetic assimilation rate as a function of intercellular CO_2 (A/C_i curves) are widely used to estimate photosynthetic parameters for C_3 species, yet few parameters have been reported for C_4 plants, because of a lack of estimation methods. Here, we extend the framework of widely-used estimation methods for C_3 plants to build estimation tools by exclusively fitting intensive A/C_i curves (6-8 more sampling points) for C_4 using three versions of photosynthesis models with different assumptions about carbonic anhydrase processes and ATP distribution. We use simulation-analysis, out-of-sample tests, existing in vitro measurements and chlorophyll-fluorescence-measurements to validate the new estimation methods. Of the five/six photosynthetic parameters obtained, sensitivity analyses show that maximal-Rubisco-carboxylation-rate, electron-transport-rate, maximal-PEP-carboxylation-rate and carbonic-anhydrase were robust to variation in the input parameters, while day-respiration and mesophyll-conductance varied. Our method provides a way to estimate carbonic anhydrase activity, a new parameter, from A/C_i curves, yet also shows that models that do not explicitly consider carbonic anhydrase yield approximate results. The two photosynthesis models, differing in whether ATP could freely transport between RuBP and PEP regeneration processes yielded consistent results under high light, but they may diverge under low light intensities. Modeling results show selection for Rubisco of low specificity and high catalytic rate, low leakage of bundle sheath and high PEPC affinity, which may further increase C_4 efficiency.

Kew words: A/C_i curves, C_4, estimation method, nonlinear curve fitting, photosynthesis parameters, V_{cmax}, electron transport, PEP carboxylation rate, carbonic anhydrase

Abbreviations: *a*, light absorptance of leaf; A_c, Rubisco carboxylation assimilation rate; *AEE*, RuBP carboxylation and PEPc carboxylation limitation assimilation; *AET*, RuBP regeneration and PEP carboxylation limitation assimilation; A_g, gross CO_2 assimilation rate per unit leaf area; A_j, RuBP regeneration assimilation rate; A_n, net CO_2 assimilation rate per unit leaf area; *ATE*, RuBP carboxylation and PEPc regeneration limitation assimilation; *ATT*, RuBP regeneration and PEPc regeneration limitation assimilation; α, the fraction of O_2 evolution occurring in the bundle sheath; *c*, scaling constant for temperature dependence for parameters; *CaL*, Lower boundary CO_2 under which assimilation is limited by RuBP carboxylation and PEPc carboxylation; *CaH*, Higher boundary CO_2 above which assimilation is limited by RuBP regeneration and PEPc regeneration; C_{bs}, bundle sheath CO2 concentration; C_i, intercellular CO_2 concentration; C_m, mesophyll CO2 concentration; ΔH_a, energy of activation for temperature dependence for parameters; ΔH_d, energy of deactivation for temperature dependence for parameters; ΔS, entropy for temperature dependence for parameters; ϕ_{PSII}, quantum yield; $\gamma^*(25)$, the specificity of Rubisco at 25°C; g_{bs}, bundle sheath conductance for CO_2; g_{bso}, bundle sheath conductance for O_2; g_m, mesophyll conductance for CO_2; *I*, light intensity; $J_{max}(25)$, maximum rate of electron transport at 25°C; $K_c(25)$, Michaelis-Menten constant of Rubisco activity for CO_2 at 25°C; $K_o(25)$, Michaelis-Menten constants of Rubisco activity for O_2; $K_p(25)$, Michaelis-Menten constants of PEP carboxylation for CO_2; O_{bs}, O_2 concentration in the bundle sheath cells; Q_{10} for K_p, temperature sensitivity parameter for K_p; *R*, the molar gas constant; R_d, daytime respiration; R_{dbs}, daytime respiration in bundle sheath cells; R_{dm}, daytime respiration in mesophyll cells; Rubisco, ribulose-1,5-bisphosphate carboxylase/oxygenase; RuBP, ribulose-1,5-bisphosphate; T_k, leaf absolute temperature; V_c, velocity of Rubisco

61 carboxylation; $V_{cmax}(25)$, maximal velocity of Rubisco carboxylation at 25°C; V_p, PEP

62 carboxylation; V_{pc}, PEPc reaction rate; $V_{pmax}(25)$, maximal PEP carboxylation rate at 25°C;

63 V_{pr}, PEP regeneration rate; x, the maximal ratio of total electron transport could be used for

64 PEP carboxylation.

65

1. INTRODUCTION

Key photosynthetic parameters allow for the assessment of how biochemical and biophysical components of photosynthesis affect net carbon assimilation in response to environmental changes, phenotypic/genotypic differences, and genetic modification. The changes in net assimilation (A_n) that occur along with the changes of intercellular CO_2 concentration (C_i) —or A/C_i curves— are widely used to estimate photosynthetic parameters for C_3 species. In particular, the method by Sharkey et al. (2007), based on the C_3 photosynthesis model of Farquhar et al. (1980; FvCB model), has been one of the most widely used tools since it is based exclusively on A/C_i curves, which are easy to measure in both lab and field conditions.

Fewer estimates of photosynthetic parameters have been reported for C_4 species, as there has been a lack of accessible C_4 estimation methods. Several recent studies, however, used A/C_i curves to estimate photosynthesis parameters based on the C_4 photosynthesis model of von Caemmerer (2000) (Ubierna et al., 2013; Bellasio et al., 2015). These studies use partial A/C_i curves; measuring assimilation rates for only a few CO_2 concentrations coupled with ancillary measurements of chlorophyll fluorescence and/or 2% O_2. While these estimation methods lead to estimates of photosynthetic parameters, the additional measurements they require make estimation more cumbersome for field work or large-scale sampling. Theoretically, it is possible to estimate photosynthetic parameters by exclusively fitting A/C_i curves to a C_4 photosynthesis model. In this paper, we propose the method to estimate C_4 photosynthesis parameters using only A/C_i curves.

There are several potential problems with A/C_i –based estimation methods for C_3 plants that carry over to existing C_4 methods (Gu et al. 2010); it is therefore important to develop a C_4 estimation method with improvements to solve the general problems and drawbacks outlined below. First, the structure of the FvCB model makes it easy to be over-parameterized. Second, a general shortcoming for the estimation methods is that they require an artificial assignment of the RuBP regeneration and Rubisco carboxylation limitation states to parts of the A/C_i curves (Xu and Baldocchi, 2003; Ethier et al., 2006; Ubierna et al., 2013; Bellasio et al., 2015), which has turned out to be problematic (Type I methods) (Gu et al. 2010). These methods assume constant transition points of limitation states for different species. Furthermore, Type I methods tend to minimize separate cost functions of different limitation states instead of minimizing a joint cost function. Some recent estimation methods for C_3 species ameliorate these problems by allowing the limitation states to vary at each iterative step of minimizing the cost function (Type II methods; Dubois et al., 2007; Miao et al., 2009; Yin et al., 2009; Gu et al., 2010). However, for these type II methods, additional degrees of freedom in these "auto-identifying" strategies can lead to over-parameterization if limitation states are allowed to change freely for all data points. Gu et al. (2010) also pointed out that existing Type I and Type II methods fail to check for inadmissible fits, which happen when estimated parameters lead to an inconsistent identification of limitation states from the formerly assigned limitation states. More specifically to C_4, the recently developed C_4 estimation methods artificially assign limitation states for A/C_i curves (Ubierna et al., 2013; Bellasio et al., 2015) and also did not check for inadmissible fits.

We developed methods to estimate photosynthetic parameters for C_4 species based solely on

fitting intensive A/C_i curves to a C_4 photosynthesis model (von Caemmerer, 2000). The intensive A/C_i curves (A/C_i curves with 6-8 more sampling points than the common A/C_i for C_3 species) are important for two reasons: First, at low C_i, the slope of A/C_i is very steep and the assimilation rate saturates quickly. Second, C_4 species have more photosynthetic parameters as the carbon concentrating mechanism adds complexity. Additionally, carbonic anhydrase catalyzes the first reaction step for C_4 photosynthesis (Jenkins et al., 1989), and it has been commonly assumed to not limit CO_2 uptake in estimation methods and C_4 models (von Caemmerer, 2000; Yin et al., 2011b). Recent studies, however, showed evidence of potential limitation by carbonic anhydrase (von Caemmerer et al., 2004; Studer et al., 2014; Boyd et al., 2015; Ubierna et al., 2017).

Therefore, first, we built estimation methods using two different fitting procedures of Sharkey et al. (2007) and Yin et al. (2011b) without considering carbonic anhydrase activity. Then, we add carbonic anhydrase limitation into the estimation method. We can also use this approach to examine how the carbonic-anhydrase-limitation assumption impacts parameter estimation, and whether the modeling of C_4 photosynthesis can be simplified by omitting it. All together, our method estimates five to six photosynthesis parameters: (1) maximum carboxylation rate allowed by ribulose 1,5-bisphosphate carboxylase/oxygenase (Rubisco) (V_{cmax}), (2) rate of photosynthetic electron transport (J), (3) day respiration (R_d), (4) maximal PEP carboxylation rate (V_{pmax}), (5) mesophyll conductance (g_m), and optionally (6) the rate constant for carbonic anhydrase hydration activity (k_{CA}). These approaches yield the following improvements to eliminate common problems occurring in the previous C_3 and C_4 estimation methods: avoiding over-parameterization, maximizing joint cost function, freely

135 determining transition points instead of assigning in advance, and checking for inadmissible
136 fits. Second, since both RuBP regeneration and PEP regeneration need ATP (Hatch, 1987),
137 we also examine two different assumptions about ATP distribution between RuBP
138 regeneration and PEP regeneration in C_4 photosynthesis models. Third, we validate the
139 estimation methods in four independent ways, using: (i) simulation tests using A/C_i curves
140 generated using our model with known parameters and adding random errors, (ii) out of
141 sample test, (iii) existing in vitro measurements and (iv) Chlorophyll fluorescence
142 measurement. Finally, we used the C_4 photosynthesis model to perform sensitivity analyses
143 and simulation analyses for important physiological input parameters. These analyses allow
144 us to illustrate the underlying physiological significance of these parameters to the ecology
145 and evolution of the C_4 photosynthesis pathway.
146

147 **2. MATERIALS and METHODS**

148 **2.1 C_4 Mechanism**

149 The CO_2 concentrating mechanism of C_4 pathway increases CO_2 in the bundle sheath cells
150 to eliminate photorespiration. Like the C_3 pathway, the diffusion of CO_2 starts from the
151 ambient atmosphere through stomata into intercellular spaces, and then into the mesophyll
152 cells. In the mesophyll cells, the first step is the hydration of CO_2 into HCO_3^- by carbonic
153 anhydrase. PEPC, then, catalyze HCO_3^- and PEP into C_4 acids and the C_4 acids are
154 transported to the bundle sheath cells. In the bundle sheath cell, C_4 acids are decarboxylated
155 to create a high CO_2 environment for the C_3 photosynthetic cycle, and PEP is regenerated.
156 All the modeling equations and mechanistic processes used for our estimation method are
157 from von Caemmerer (2000), Hatch and Burnell (1990), Boyd et al. (2015) and Ubierna et

158 al. (2017) (Supplementary Methods).

159

160 Given the two limitation states of C_4 cycle (PEP carboxylation (V_{pc}) and PEP Regeneration
161 (V_{pr})), and two limitation states of C_3 cycle (RuBP carboxylation (A_c) and RuBP
162 Regeneration (A_j)) in the C_4 photosynthesis model, there are four combinations of limitation
163 states (as Yin et al., 2011b, Fig. 1): RuBP carboxylation and PEP carboxylation limited
164 assimilation (AEE), RuBP carboxylation and PEP regeneration limited assimilation (ATE),
165 RuBP regeneration and PEP carboxylation limited assimilation (AET) and RuBP
166 regeneration and PEP regeneration limited assimilation (ATT). Since the C_4 cycle operates
167 before the C_3 cycle and provides substrates for the C_3 cycle, the determination process of A_n
168 is as follows:

169 $$\text{If } (V_{pc} < V_{pr}), A_c = AEE, A_j = AET, \text{otherwise } A_c = ATE, A_j = ATT \quad (1)$$

170 $$A_n = \min(A_c, A_j), \quad (2)$$

171 which we used for our estimation method.

172

173 **2.2 Plant Material**

174 We performed intensive A/C_i curves on nine different C_4 species to develop and examine the
175 efficacy of our estimation tools: *Zea mays* L., *Eragrostis trichodes* (Nutt.) Alph. Wood,
176 *Andropogon virginicus* L., *Schizachyrium scoparium* (Michx.) Nash, *Panicum virgatum* L.,
177 *Panicum amarum* Elliott, *Setaria faberi* Herrm., *Sorghastrum nutans* (L.) Nash
178 and *Tripsacum dactyloides* (L.) L. The intensive A/C_i curves contain more sample points
179 under more CO_2 concentrations than the default curve used for C_3 species. Here we set the
180 CO_2 concentrations as 400, 200, 50, 75, 100, 125, 150, 175, 200, 225, 250, 275, 300, 325,

350, 400, 500, 600, 700, 800, 1000, 1200, 1400 ppm under light intensity of 1500 μmol$m^{-2}s^{-1}$ (light intensity encountered by the plants in greenhouse). At each point, data was recorded when the intercellular CO_2 concentration equilibrated within 2-5 minutes. The datasets were obtained using a standard 2 x 3 cm^2 leaf chamber with a red/blue LED light source of LI-6400 (LI-COR Inc., Lincoln, NE, USA). If the stomatal conductance of a species does not decrease quickly at high CO_2, then the sample points at the high CO_2 level can be increased. Fluorescence was measured along with A/C_i curves for seven C_4 species (CO_2 concentration is similar with above). After each change of CO_2 concentration and A reached steady state, the quantum yield was measured by multiphase flash using a 2 cm^2 fluorescence chamber head (Bellasio et al., 2014). All the measurements are conducted at 25°C and VPD is controlled at 1-1.7kPa. The cuvette was covered by Fun-Tak to avoid and correct for the leakiness (Chi et al., 2013).

2.3 Estimation Protocol

We implemented the estimation methods using the non-linear curve-fitting routine in MS Excel (Supplementary Material I, II, III) and independently in R ("C4Estimation") to get solutions that minimize the squared difference between observed and predicted assimilation rates (A). Five (or six when considering carbonic anhydrase) parameters will be estimated by fitting the A/C_i curve: V_{cmax}, J, R_d, V_{pmax}, g_m, and $k_{CA.}$ Other input parameters for C_4 are in Table S1.

Input data sets and preliminary calculations. The input data sets are the leaf temperature during measurements, atmosphere pressure, two CO_2 bounds (*CaL* and *CaH* discussed in the

following section), and the assimilation rates (A) and the C_is (in ppm) in the A/C_i curve. Also, reasonable initial values of output parameters need to be given in the output section to initiate the non-linear curve fitting (Supplementary Material IV). C_i will be adjusted from the unit of ppm to the unit of Pa inside the program as suggested by Sharkey et al. (2007).

Estimating limitation states. We set upper and lower limits to the value of C_i between which the assimilation rates are freely determined by limitation states. Also, we can avoid over-parameterization by pre-assigning limitation states at the lower and upper ends of the C_i range. We assumed that under very low C_i (*CaL*), CO_2 is the limiting substrate; thus, V_p is limited by V_{pc} and A is given by A_c (AEE); under very high C_i (*CaH*) electron transport is limiting, thus, V_p is limited by V_{pr} and A is given by A_j (ATT) (Fig. 1). The points between *CaL* to *CaH* are freely determined by AEE, ATE, AET or ATT from eq. (16) and (17) to minimize the cost function. We suggest setting *CaL* as 10 Pa initially, then adjusting based on the preliminary results. The points of constant A at high C_i end can initially be set as being limited by ATT primarily (based on the three points, we can *CaH*) or use 65 Pa as the first trial. The range of freely determined points can be adjusted by users by setting appropriate *CaL* and *CaH*. In the column of "Estimate Limitation", whether the data points are limited by AEE (represented by "1"), ATT (represented by "4") or freely vary (represented by "0"), all the assignments of "1", "4" and "0" are determined automatically by the given values of *CaL* and *CaH*. One can input "-1" to disregard a data pair. Users can adjust limitation states according to how many points and the range of C_i they have in their A/C_i curves.

We assume different processes in the C_4 photosynthesis are coordinated with each other and co-limit the assimilation rate (Sharkey et al., 2007; Yin et al., 2011b; Ubierna et al., 2013; Bellasio et al., 2015). Thus, the estimation parameters allow the limitation states to be compactly clustered with each other (Fig. 1). However, if there were only a few points under *CaL*, the estimation results will depend heavily on the given initial values and unbalanced results would be more likely. Fig. S1 shows an example of unbalanced estimation results by deleting some points under 10 Pa or setting a very low *CaL*: in the estimation results, A_n is limited by *AEE* at very low C_i and is mostly limited by A_j (shown by AET and ATT) in the C_3 cycle. In this case, A_c (shown by AEE and ATE) has a clear redundancy at higher C_i. Unbalanced results happened when there are not enough constraints points under *CaL* or above *CaH*. Such results explain why intensive A/C_i curves are preferred, especially more measuring points under the lower end and higher end of C_i. However, existing A/C_i data with 14 points might be used in the current estimation method if there are at least four points below *CaL* and three points above *CaH*.

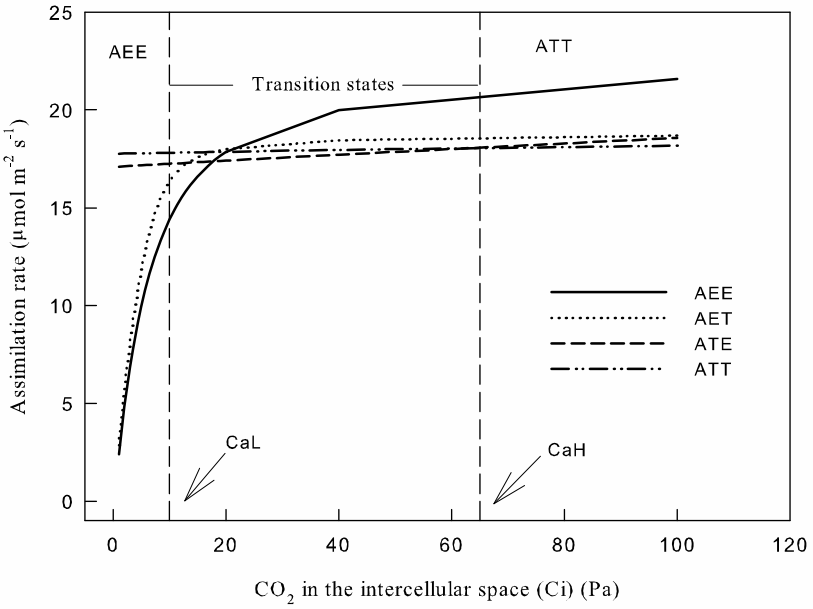

Fig. 1 An introduction of how our estimation methods assign transition points between limitation states. AEE represents RuBP carboxylation, and PEP carboxylation limited assimilation rate, ATT represents RuBP regeneration and PEP regeneration limited assimilation rate. Transition states indicate assimilation could be limited by AEE, ATT, ATE (RuBP carboxylation and PEP regeneration) and AET (RuBP regeneration and PEP carboxylation). Our algorithm allows the transition states to be freely limited by the above four conditions from a lower bound (*CaL*, 10 Pa for instance) and a higher bound (*CaH*, 65 Pa for example), indicated by the dashed vertical lines in the figure.

Estimation algorithm and fitting procedures. The objective of our estimation methods is to minimize the following joint cost function (eq. 3 and 4) by varying the above five or six output parameters (V_{cmax}, J, R_d, V_{pmax}, g_m, and k_{CA}):

$$f = \sum_{i=1}^{n} (A_i - A_{mi})^2. \quad (3)$$

$$A_i = [If(C_i \leq CaL), AEE; If\ (C_i \geq CaH), ATT; IF\ (CaL \leq C_i \leq CaH), \min(A_{ci}, A_{ji})] \quad (4)$$

n is the total number of observations, A_{ci} is determined by AEE and ATE and A_{ji} is determined by AET and ATT from eq. (1), A_{mi} is the observed net assimilation rate.

In this calculation, we take Michaelis-Menten constant of Rubisco activity for CO_2 (K_c), Michaelis-Menten constant of Rubisco activity for O_2 (K_o), the specificity of Rubisco (γ*), Michaelis-Menten constants of PEP carboxylation for CO_2 or $HCO3^-$ (K_p), the fraction of O_2 evolution occurring in the bundle sheath (α) and bundle sheath conductance (g_{bs}) as given (input parameters), similar to Sharkey et al. (2007). We conduct further sensitivity analyses in the following section to determine the effects of variability of these inputs parameters on the estimation results.

We used two fitting procedures in the current study: one was from Sharkey et al. (2007), which is an implicit minimization of error (Supplementary Material I, III), and the other one was based on the explicit calculations given by Yin et al. (2011b) (Supplementary Material II). For the method of Sharkey et al. (2007), ”estimated” A_n was calculated using the above equations and observed A_n values. We call them ”estimated”, because when we calculate A_n, observed A_n is used to calculate intermediate parameters, for example, the CO_2 concentration in mesophyll cells (C_m), the CO_2 concentration in bundle sheath (C_{bs}), which we then use to calculate A_c and A_j. The objective function is to minimize the sum of square errors between ”estimated” A_n and observed A_n (Simulation Error in Supplementary Material I, III). For the model without carbonic anhydrase, Yin et al. (2011b) gave explicit solutions for AEE, ATE, AEE, and ATT). “Explicit” here means the assimilation rates are totally calculated by the estimated parameters without calculating the intermediates with observed A_n. These calculations give us the real estimation error of our fitting procedure for models without carbonic anhydrase and thus provide a validation for the goodness of fit (“True Error” in Supplementary Material I-III).

Checking inadmissible fits. We made it possible to check the inadmissible fits for limitation states in our estimation method. After the estimation process finishes, the limitation states based on the estimated parameters will be calculated in the last column. If the calculated limitation states are inconsistent with the assigned ones in the estimation method, one needs to readjust the assignment of the “Estimate Limitation” (adjust *CaL* or *CaH*) and rerun the estimation method, until they are consistent with each other.

288

289 **3. RESULTS**

290 **3.1 Estimation results and assumptions**

291 Estimation methods based on assumptions with and without carbonic anhydrase yield
292 similar results (Supplementary material V). In Supplementary material III, carbonic
293 anhydrase indeed shows limitation to V_{pc}, which confirms its potential role as a limiting step
294 in the C_4 cycle. However, V_{pc} calculated from CO_2 are only a little higher than V_{pc} calculated
295 from HCO_3^-, which resulted in the similar estimation results. In addition, the estimation
296 errors and true errors from Yin's equations are quite small (average<1), and also similar
297 between models with and without carbonic anhydrase.

298

299 Estimation methods based on the two equations of different assumptions about electron
300 transport between RuBP regeneration and PEP regeneration yield consistent parameter
301 estimates and assimilation- CO_2 response curves (Fig. 2), but there were minor differences.
302 The second assumption that ATP, resulting from electron transport, is freely allocated
303 between PEP carboxylation-regeneration and RuBP regeneration leads to a bump at low
304 CO_2 when estimating ATE. The two assumptions produce different ATE under low CO_2; but
305 this is largely inconsequential because, under low CO_2, assimilation is usually limited by
306 AEE.

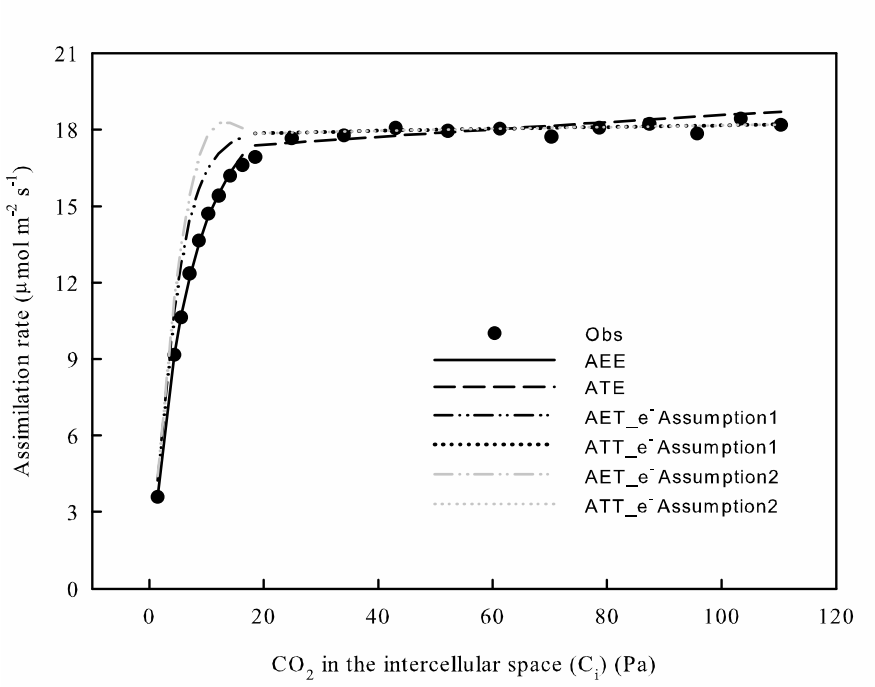

Fig. 2 Assimilation-CO_2 response curves (A/C_i) generated using C_4 photosynthesis of two different assumptions about electron transport. Photosynthetic parameters (V_{cmax}, J, R_d, V_{pmax}, and g_m) are the same for both assumptions. AET_e$^-$Assumption1 and ATT_e$^-$Assumption1 represent results of the assumption that no matter how much electron transport is used for PEP carboxylation/regeneration, a certain amount (xJ) is confined for this use. AET_e$^-$Assumption2 and ATT_e$^-$Assumption2 represent results of the assumption that electron transport can be freely distributed between PEP carboxylation/regeneration and RuBP regeneration. Parameters are estimated from A/C_i curve of *T. dactyloides* under the light intensity of 1500 μmol m^{-2} s^{-1}. AEE and ATE are the same for both assumptions.

3.2 Sensitivity analysis

The parameters K_c, K_o, γ^*, K_p, α, and g_{bs} can vary among species in nature (Cousins et al., 2010) and it is therefore important to know how sensitive our results are to variation in these parameters. We conducted a sensitivity analysis for variation in these parameters on the

estimated V_{cmax}, J, R_d, V_{pmax}, g_m and k_{CA} (Fig. 3). This analysis shows all the estimated parameters are robust under the variation of α (Fig. 3A) and showed little variation responding to the change of γ^* (Fig. 3E) and K_o (Fig. 3C); however, the estimated parameters are dependent on the other input parameters to different extents (Fig. 3B, D, F). We calculate the average percentage change of estimated parameters along with the 50 % decrease and 100 % increase of the input parameters. V_{cmax} showed some medium extent of sensitivity for K_c, K_p, and g_{bs} with the average percentage change of 23.11, 7.54 and 17.69 % respectively. J is robust in the variations of K_c, and g_{bs} (the average change is less than 2%) and with a medium 6.96 % change for K_p. k_{CA} is robust in the variations of K_c, K_p, and g_{bs} (average change less than 5%). V_{pmax} is sensitive for K_p with the average change of 27.34%, moderately sensitive to the change of g_{bs} with 4.01 % and 13.38% change and is robust for K_c. R_d is sensitive to K_c, K_p, and g_{bs} with the change of 6.73, 43.88 and 13.38%. g_m is strongly sensitive to K_c, K_p, and g_{bs} with the average percentage changes of 22.95, 107.04 and 23.19 %. This results suggest that V_{cmax}, J, V_{pmax}, and k_{CA} estimated using our method are relatively robust.

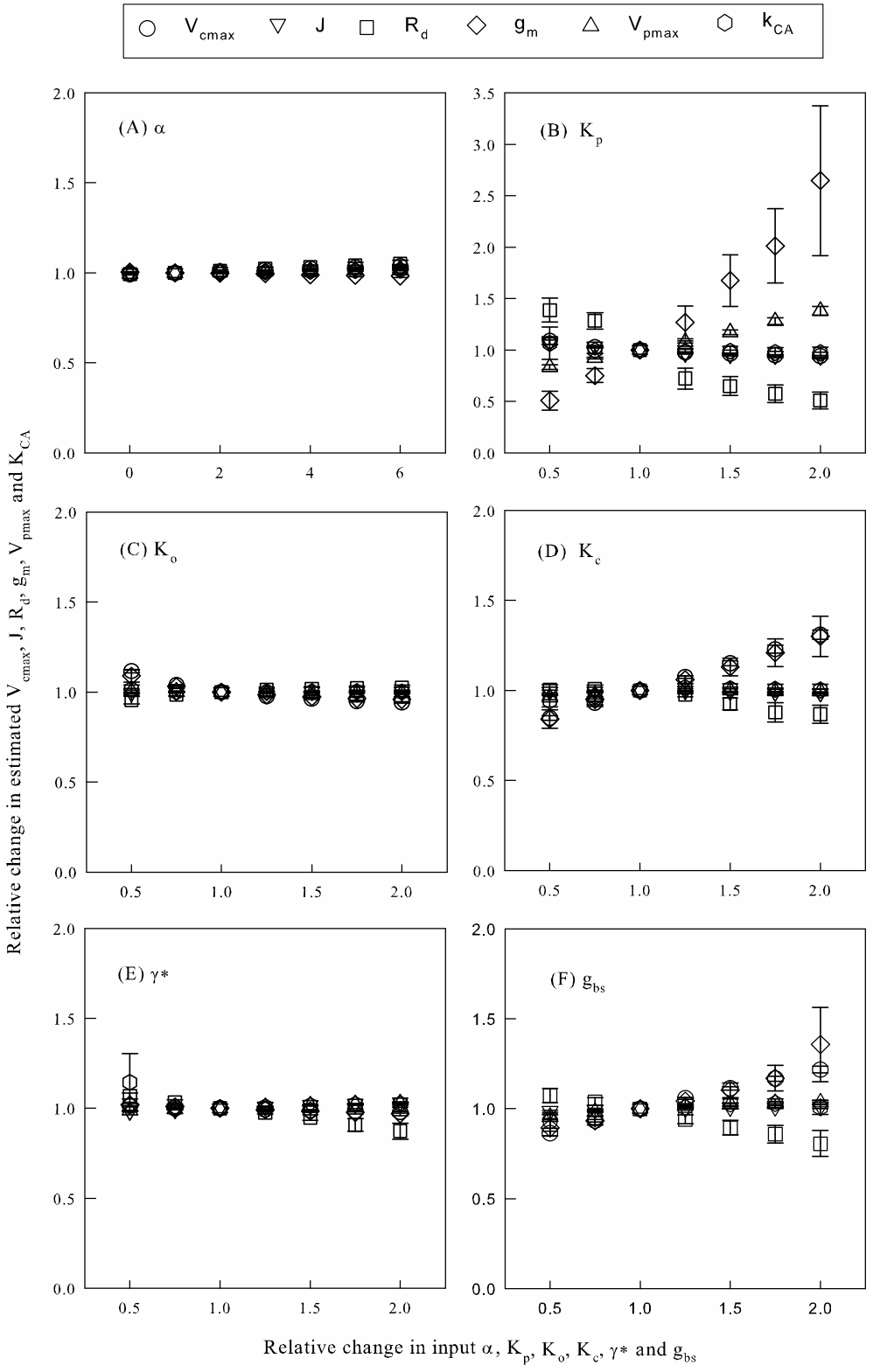

Fig. 3 Sensitivity analysis of six estimation parameters to the variation in six input parameters using the model with carbonic anhydrase. Relative changes in the estimated V_{cmax}, J, R_d, V_{pmax}, g_m and k_{CA}

in response to the relative change of six input parameters [(A) α, (B) K_p, (C) K_o, (D) K_c, (E) γ^* and (F) g_{bs}] from the initial values in Table S1. The relative change of estimated parameters refers to the ratio of estimated values at a changed input parameter to the estimated value at the initial value of that input parameter. The symbols represent the average change of the nine C_4 species and error bars represent standard error.

3.3 Physiological significance for assimilation rate of the input parameters

In addition to the sensitivity analysis, we performed a simulation analysis to illustrate the physiological importance of input parameters further, and to indicate further the importance of physiological properties in maintaining the efficiency of C_4 photosynthesis pathway. We chose the estimation parameter set of *T. dactyloides* as an example, held photosynthetic parameters constant V_{cmax} (28 μmol m^{-2} s^{-1}), J (134 μmol m^{-2} s^{-1}), R_d (0.78 μmol m^{-2} s^{-1}), g_m (30.00 μmol m^{-2} s^{-1} Pa^{-1}) and V_{pmax} (41.91 μmol m^{-2} s^{-1}), while changing the values of α, γ^*, g_{bs}, and K_p (as half or twice of the original parameters) to see their effects on the assimilation rate, C_{bs} and the O_2 concentration in bundle sheath (O_{bs}) (Fig. 4, Table 1). Using photosynthetic parameter sets of other species to perform the simulation analysis yielded similar results (data not shown). The change of α did not lead to changes in assimilation rate (Fig. 4A) and led to small changes in O_{bs} (Table 1). The decrease of γ^* to half of the current value led to a small change of C_{bs} and assimilation rate (less than 0.5 μmol m^{-2} s^{-1}) while doubling γ^* led to a larger, but still not significant, change (less than 1 μmol m^{-2} s^{-1}) (Fig. 4B, Table 1). Importantly, the changes of assimilation rates were less than 0.3 μmol m^{-2} s^{-1} when C_i was less than 20 Pa, which is the regular range of C_i under current ambient CO_2. However, the change of g_{bs} significantly changed the assimilation rate

363 and C_{bs} (Fig. 4C, Table 1). The change of K_p significantly affected the assimilation rate and

364 C_{bs} to a large degree under low C_i (Fig. 4D, Table 1).

365

366 **Table 1** The average change of percentage of CO_2 concentration (C_{bs}) and O_2 concentration at

367 bundle sheath (O_{bs}) compared to the reference value of $\alpha 0$, $\gamma^* 0$, $g_{bs} 0$ and K_p. Simulation results are

368 obtained by using the original parameter set of *T. dactyloides* with V_{cmax} = 28 μmol m^{-2} s^{-1}, J = 134

369 μmol m^{-2} s^{-1}, R_d = 0.78 μmol m^{-2} s^{-1}, g_m = 30.00 μmol m^{-2} s^{-1} Pa^{-1} and V_{pmax} = 41.91 μmol m^{-2} s^{-1}. The

370 values represent average change of percentage of 21 values from 0-120 Pa of intercellular CO_2 (C_i)

371 (data show mean (standard error)).

Parameters	$\alpha = 0$	$\alpha = 2\ \alpha 0$	$\gamma^* = 0.5\ \gamma^* 0$	$\gamma^* = 2\ \gamma^* 0$
Chang of C_{bs} (%)	-0.91(0.06)	0.97(0.06)	-2.96(0.28)	5.05(0.49)
Chang of O_{bs} (%)	-6.07(0.30)	6.01(0.30)	0.07(0.01)	-0.21(0.02)
Parameters	$g_{bs} = 0.5\ g_{bs} 0$	$g_{bs} = 2\ g_{bs} 0$	$K_p = 0.5\ K_p 0$	$K_p = 2\ K_p 0$
Chang of C_{bs} (%)	56.99(3.03)	-29.48(0.41)	43.12(10.75)	-36.57(4.07)
Chang of O_{bs} (%)	6.77(0.29)	-3.41(0.16)	0.91(0.18)	-1.18(0.14)

372

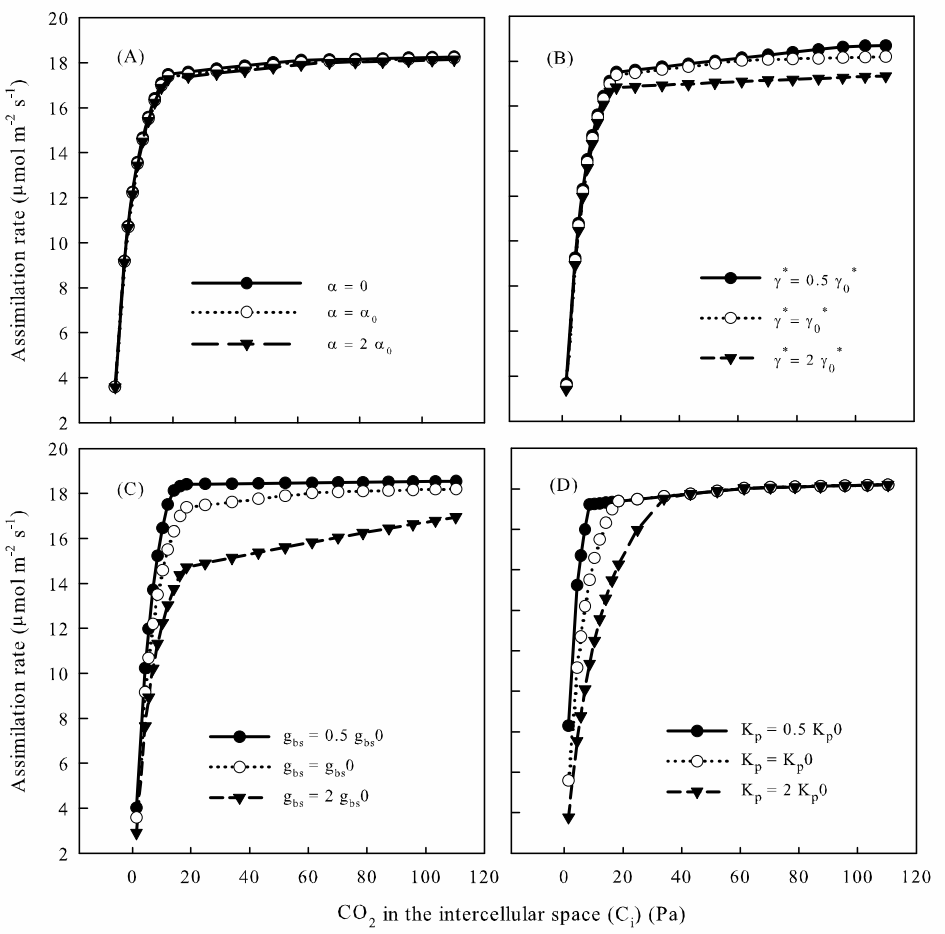

373

374 **Fig. 4** Simulation results of assimilation rate along with different intercellular CO_2 concentration (C_i)

375 with the known photosynthetic parameters, but with the change of (A) α, (B) γ^*, (C) g_{bs} and (D) K_p.

376 The original data set are V_{cmax} = 28 μmol m^{-2} s^{-1}, J = 134 μmol m^{-2} s^{-1}, R_d = 0.78 μmol m^{-2} s^{-1}, g_m =

377 30.00 μmol m^{-2} s^{-1} Pa^{-1} and V_{pmax} = 41.91 μmol m^{-2} s^{-1}. The reference value of changing parameters at

378 25°C: α0(25) = 0.15, γ^*0(25) = 0.000244, g_{bs}0(25) = 0.0295 and K_p(25) = 8.55 Pa.

379

380 **3.4 Validating the estimation methods**

381 In order to test our estimation methods, we first conducted a simulation test with

382 manipulated error terms. We use the estimated results of the nine species as known

383 parameters (the known values in Fig. 5) to generate new datasets using the C_4

384 photosynthesis equations based the first assumption of electron transport and adding error
385 terms to the assimilation rates. The error terms were randomly drawn from a normal
386 distribution of mean zero and standard deviation of 0.1 or 0.2 in an effort to simulate the
387 inevitable random errors in the real measurements. Estimating simulated data sets gave us an
388 idea about how likely we can capture the real parameters of the species given unavoidable
389 errors in measurements. The results show that robust estimation results for V_{cmax}, J, V_{pmax},
390 and R_d can be obtained (Fig. 5A, B, C, D). However, some estimation results of g_m and k_{CA}
391 show some deviation from the real values (Fig. 5E, F).
392
393 To test whether our estimation method could give accurate predictions across typical
394 prediction scenarios, (CO_2 ranging from 20 Pa to 60 Pa), we performed out of sample tests
395 for our nine target species. To perform these tests, we removed five points of CO_2
396 concentrations between 20 and 60 Pa range out of the A/C_i curves and used the rest of the
397 A/C_i curves to estimate parameters. And then we used these parameters to predict the
398 assimilation rate under the CO_2 concentrations we took out before and calculated the
399 estimation errors. In general, the estimation errors for all our species were small (Table 2).
400
401 **Table 2** Out of sample test results. Five measured points from 20 Pa-60 Pa were taken out when we
402 conducted the estimation process. Then the calculated assimilation rates under these five CO_2
403 concentrations were compared with the measured ones. The data shows estimated error between the
404 calculated and measured assimilation rates (data show mean (standard error)).

Species	*A. virginicus*	*Z. mays*	*E. trichodes*	*P. virgatum*	*P. amarum*
Model without CA	0.069(0.036)	0.150(0.056)	0.035 (0.017)	0.193(0.063)	0.055(0.034)
Model with CA	0.066(0.043)	0.154(0.057)	0.111 (0.058)	0.195 (0.061)	0.054(0.033)

Species	*S. scoparium*	*S. faberi*	*S. nutans*	*T. dactyloides*
Model without CA	0.023(0.010)	0.114(0.055)	0.258(0.080)	0.199(0.090)
Model with CA	0.105(0.034)	0.068(0.040)	0.263(0.133)	0.200(0.090)

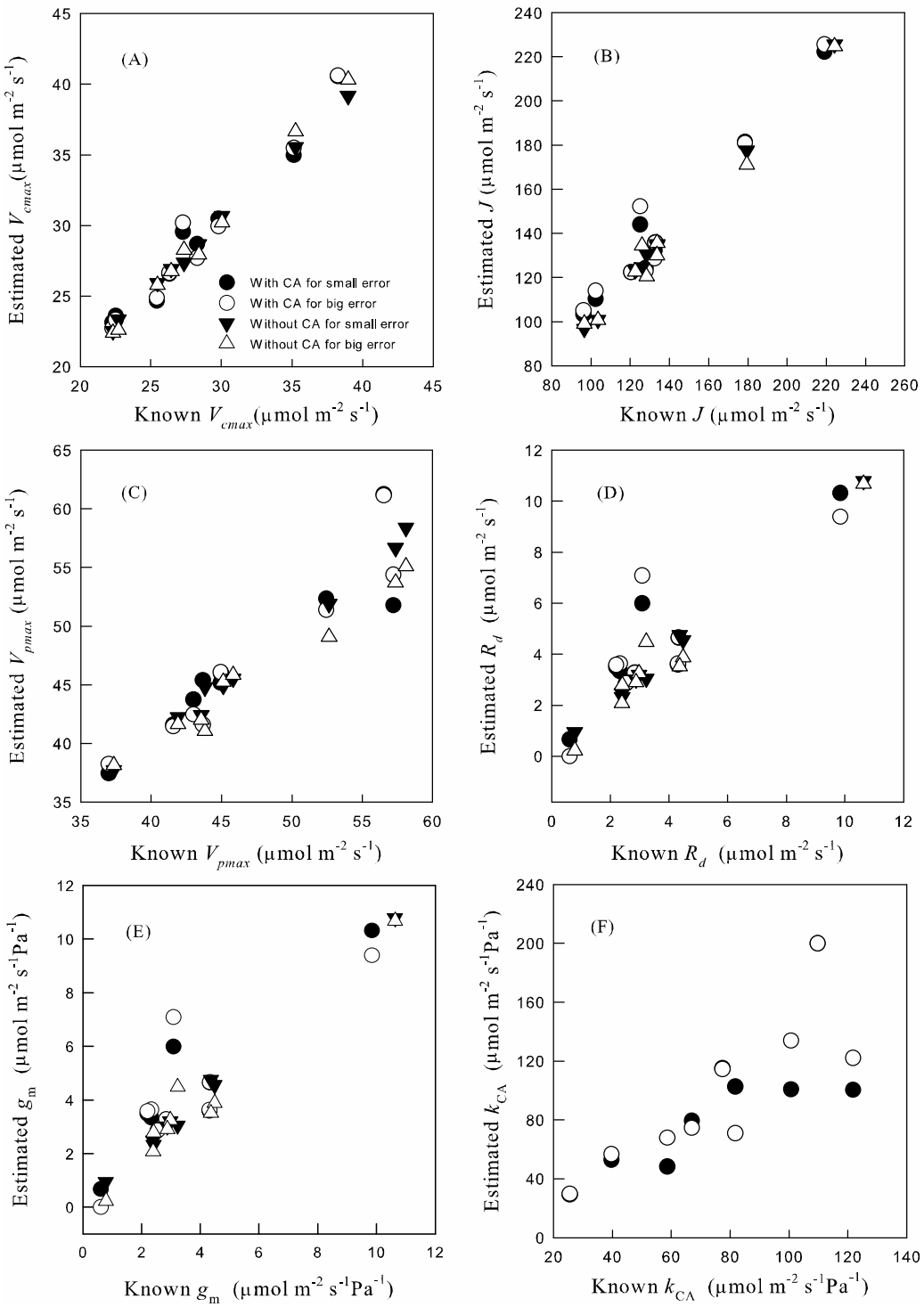

409 **Fig. 5** Simulation tests for the estimated parameters ((A) V_{cmax}, (B) J, (C) V_{pmax}, (D) R_d, (E) g_m and
410 (F) k_{CA}) using estimation methods with and without carbonic anhydrase reaction (With CA and
411 Without CA). Datasets are generated by adding random errors for the modeling results using the
412 known photosynthesis parameters of nine species. These known photosynthesis parameters are the
413 true values in the x-axis and are used to compare with the newly estimation parameters. The small
414 error refers to error term randomly chosen with mean 0 and standard deviation of 0.1 and the bigger
415 error refers to error term with randomly chosen mean 0 and standard deviation of 0.2.
416
417 We tried to compare our estimation methods with in vitro measurements or other estimation
418 methods using isotopic analysis, especially for *Zea*. Our estimation results for *Zea* obtained
419 similar V_{cmax} with the in vitro estimated Rubisco activity of Pinto et al. (2014); however, the
420 estimated value for V_{pmax} is a little lower than the in vitro PEPC activity measurement with a
421 difference of around 10 μmol m^{-2} s^{-1}. For species of the Panicum family with NAD-ME
422 subtype, *P. virgatum* and *P. amarum* in the current study and *P. coloratum* in Pinto et al.
423 (2014), the estimated V_{cmax} and V_{pmax} are quite consistent with the in vitro measurements.
424 Ubierna et al. (2017) reported the g_m for *Zea* ranged from 1.69 ± 0.17 to 8.19 ± 0.80 μmol
425 m^{-2} s^{-1} Pa^{-1} using ^{18}O and in vitro V_{pmax}. Our estimation method fitted a g_m for *Zea* of 7.34
426 μmol m^{-2} s^{-1} Pa^{-1}, which falls into the range of their measurements. Barbour et al. (2016)
427 reported a little lower mesophyll conductance for *Zea* using ^{18}O measurements.
428
429 **3.5 Validating transition point range**
430 We used chlorophyll fluorescence measurements from seven C_4 species to test whether the
431 upper and lower boundary CO_2 concentrations, *CaL* and *CaH*, are reasonable (Table 3). The
432 apparent quantum efficiency of PSII electron transport was calculated with $\Delta F/F_m' = (F_m' -$

433 F_S) F_m' (Genty, Briantais & Baker 1989). Fluorescence analysis (Baker et al. 2007) is a
434 powerful tool for identifying the limitation states of C_3 species (Sharkey et al. 2007). If
435 Chlorophyll fluorescence is increasing with increasing CO_2, A_n is limited by Rubisco
436 carboxylation limited; when Chlorophyll fluorescence stays constant with increasing CO_2,
437 A_n is limited by RuBP regeneration. For C_4 species, however, the situation is more
438 complicated. Since V_p could be limited by V_{pr} and V_{pc} (eq. (9)). Part of the RuBP
439 carboxylation limited condition and RuBP regeneration limited condition for the C_3 cycle
440 will mix together, leading to a linear increase of fluorescence with increasing of CO_2, but of
441 a small slope (Fig. S2). Thus, we can only obtain two boundaries of CO_2 concentrations.
442 Below the lower boundary, *A* and fluorescence increases with increasing C_i with a steep
443 slope and *A* is RuBP carboxylation and PEP carboxylation limited (AEE); above the higher
444 boundary, *A* and fluorescence is relatively constant along with the increase of C_i and *A* is
445 RuBP regeneration and PEP regeneration limited (ATT). We measured fluorescence to test
446 whether the upper and lower boundary CO_2 concentrations, *CaL* and *CaH*, are reasonable. It
447 seems all the *CaL* are above 14 Pa and all the *CaH* are below 65 Pa (Table 3). These results
448 suggest that 10Pa-65Pa is a reasonable range for the transitional point.
449
450 **Table 3** CO_2 concentration boundaries result for assimilation-limited conditions from fluorescence
451 measurements for seven species. Low: CO_2 concentration under which assimilation rate increases
452 greatly with increasing CO_2 (potentially assimilation is limited by PEP carboxylation and RuBP
453 carboxylation). High: CO_2 concentration above which assimilation rate no longer increases with
454 increasing CO_2 (potentially assimilation is limited by PEP regeneration and RuBP regeneration).
455 Data show the mean (standard error).

Species	*P. virgatum*	*P. amarum*	*S. scoparium*	*S. nutans*

Low(Pa)	14.1(1.12)	18.0(1.09)	17.8(1.09)	17.6(0.28)
High(Pa)	34.1(1.78)	55.5(1.40)	53.1(1.10)	63.1(2.07)

Species	*T. dactyloides*	*T. flavus*	*B. mutica*
Low(Pa)	13.8(0.35)	14.9(2.35)	15.8(1.13)
High(Pa)	46.1(0.20)	41.4(1.73)	42.3(1.24)

4. DISCUSSION

The photosynthetic parameters from the estimation method are good indicators for the biochemical and biophysical mechanisms underlying the photosynthesis processes of plants. Together with photosynthesis models, they can provide powerful information for evolutionary and ecological questions in both physiological and ecosystem response to natural environmental variation and climate change, to illustrate evolutionary trajectory of C_4 pathway, as well as in efforts to improve crop productivity (Osborne & Beerling, 2006; Osborne & Sack, 2012; Heckmann et al., 2013). Photosynthetic parameters represent different physiological traits, and comparison of these parameters within a phylogenetic background could help us to understand the further divergence of lineages and species through evolutionary time. Additionally, the response of productivity and carbon cycle of vegetation towards the future climate change depends heavily on photosynthesis parameter estimation as input parameters.

Each of the two different fitting procedures has advantages and disadvantages. Yin's method (Supplementary material II) uses the explicit calculation of assimilation rate and consequently gives lower estimation error. However, it needs a more accurate assignment of limitation states, especially at the lower end. Thus, Yin's method will be preferable if one

has additional support (e.g. fluorescence measurement) to define the limitation states; otherwise, the Yin's method may give unbalanced results (Fig. 3). However, Sharkey's method (Supplementary material I) usually can avoid unbalanced results even without ancillary measurements. Thus, it is better to use both procedures to support each other to find more accurate results. For example, one can first use Sharkey's method to get estimation results and limitation states, and then use them as initial values for Yin's method.

Our estimation methods yielded similar results when using models with and without carbonic anhydrase reaction processes. Although carbonic anhydrase activity may well be a limiting step for C_4 cycle (von Caemmerer et al., 2004; Studer et al., 2014; Boyd et al., 2015; Ubierna et al., 2017), its limitation did not greatly affect assimilation rates in this study. Including the carbonic anhydrase reaction makes the model more complex and difficult to get an explicit solution; therefore, the model without carbonic anhydrase could be used as a simplified form yielding flawed but 'nearly correct' predicted values as a part of larger models. However, carbonic anhydrase limitation of C_4 photosynthesis needs the further assessment from physiological or biochemical perspectives, and our estimation method provides another way to derive carbonic anhydrase parameters, which were comparable with *in vitro* measurements (Boyd et al., 2015). In addition, our results for models with and without carbonic anhydrase activity support the proposition of Cousins et al. (2007) that carbonic anhydrase activity may not be a limiting factor for A/C_i curves of C_4 plants.

Our results show that despite a clear difference between the assumptions of how the

498 products of electron transport are distributed, the results were similar and comparable with
499 studies using different models under measurements of high light intensity. The bump in the
500 second model happens in AET. In AET, assimilation is limited by RuBP regeneration and
501 PEP carboxylation; therefore, PEP regeneration is not reaching V_{pr}, and the extra electron
502 transport in PEP regeneration could be freely assigned to RuBP regeneration. This effect
503 will weaken as PEP carboxylation increases. However, under lower photosynthetic photon
504 flux density, assimilation rate will be limited more by electron transport, and the separate
505 assumptions concerning electron transport may start to show divergent results.
506
507 The photosynthetic parameters from the estimation method used together with
508 photosynthesis models can provide information and inspiration about the evolutionary and
509 physiological importance of different aspects of the C_4 syndrome (Osborne & Sack, 2012;
510 Heckmann et al., 2013), which can be investigated by empirical measurements. Several
511 examples emanate from our simulation analysis: (1) α represents the fraction of O_2
512 evolution from photosynthesis occurring in the bundle sheath cells (eq. (4)) and any $\alpha > 0$
513 means that O_2 will accumulate in the bundle sheath cells, due to low g_{bs} Both the sensitivity
514 analysis and the simulation analysis showed the change of α did not affect the estimated
515 parameters and assimilation rates, because the high C_{bs} created by C_4 carbon concentrating
516 mechanism overcame any increase of O_{bs} and did not lead to high photorespiration. Thus,
517 the compartmentation of O_2 evolution may not have played an important role in the
518 evolution of C_4 photosynthesis. (2) A lower Rubisco specificity factor (γ^*;eq. (11)) means
519 lower specificity for O_2, higher specificity for CO_2, and lower photorespiration. In C_3
520 species, selection for Rubisco with lower specificity to O_2 and high specificity of CO_2 can

increase the carbon gain. However, there is a trade-off between the specificity of Rubisco for CO_2 and its catalytic rate (Savir et al., 2010; Studer et al., 2014). Based on this trade-off, we can hypothesize that since C_4 elevates CO_2 around Rubisco relative to the O_2 concentration, maintaining low specificity might be optimal, in order to get high catalytic rate of the enzyme to reach higher assimilation rate as shown by the empirical measurements of Sage (2002) and Savir et al. (2010). Our simulation analysis showed the increase of specificity for CO_2 (decrease of γ^*) did not increase the assimilation rate much, which indicates the selection upon Rubisco specificity in C_4 plants should be relaxed. (3) g_{bs} represents CO_2 leakage from bundle sheath to the mesophyll cell, and changes in g_{bs} significantly change the assimilation rate and C_{bs}. Therefore, avoiding CO_2 leakage was of great importance for the evolution and efficiency of C_4 photosynthesis pathway (Brown and Byrd, 1993; Ubierna et al., 2013; Kromdijk et al., 2014).

Although we have shown that parameter estimation can be achieved solely with A/C_i curves, it is easy to combine our methods with ancillary measurements to yield more accurate estimation results by defining the parameters as estimated or known or add additional constraints (Supplementary Material IV). Yin et al. (2011b) proposed a method to obtain R_d from the fluorescence-light curve, since the method used for C_3 species, the Laisk method, is inappropriate (Yin et al., 2011a). Additional measurement of dark respiration could be an approximation for R_d or could help to provide a constraint for estimating R_d in our estimating method. Ubierna et al. (2017) discussed the estimation method of g_m using instantaneous carbon isotope discrimination. With external measurement results, one can change estimated parameters (such as R_d, g_m and J) as input parameters, instead of output

544 parameters, in this curve fitting method (Supplementary material IV). Additional methods,
545 such as in vitro measurements (Boyd et al., 2015; Pedomo et al., 2015) and membrane inlet
546 mass spectrometry (Cousins et al., 2010) of V_{cmax}, V_{pmax}, and carbonic anhydrase activity can
547 also provide potential parameter values. Furthermore, if some output parameters are
548 determined in the external measurements, one can also relax the input parameters (such as
549 g_{bs}) and make them estimated parameters (Supplementary material IV).
550

551 **5. Conclusion**

552 We have developed new, accessible estimation tools for extracting C_4 photosynthesis
553 parameters from intensive A/C_i curves. Our estimation method is based on an established
554 estimation protocol for C_3 plants and makes several improvements upon C_4 photosynthesis
555 models. External measurements for specific parameters will increase the reliability of
556 estimation methods and are summarized independently. We developed estimation methods
557 with and without carbonic anhydrase activity. The comparison of these two methods allows
558 for an estimation of carbonic anhydrase activity, and further shows that the method that did
559 not consider carbonic anhydrase activity was a sufficient simplification for C_4
560 photosynthesis. We tested two assumptions related to whether the electron transport is freely
561 distributed between RuBP regeneration and PEP regeneration or certain proportions are
562 confined to the two mechanisms. They show similar results under high light, but they may
563 diverge under low light intensities. Simulation test, out of sample test, fluorescence analysis,
564 and sensitivity analysis confirmed that our methods gave robust estimation especially for
565 V_{cmax}, J, and V_{pmax}.
566

Author contributions

HZ, EA and BH conceived the ideas, designed methodology, analyzed the data and led the writing of the manuscript; HZ collected the data; HZ and BH coordinate the study. All the authors contributed to the critical review of the manuscript and approved its final version.

ACKNOWLEDGMENT

We thank Dr. Jesse Nippert, Kansas State University, for providing the fluorometer chamber.

REFERENCES

Baker NR, Harbinson J, Kramer DM. 2007. Determining the limitations and regulation of photosynthetic energy transduction in leaves. Plant, Cell and Environment **30**, 1107–1125.

Barbour MM, Evans JR, Simonin KA, Von Caemmerer S 2016. Online CO_2 and H_2O oxygen isotope fractionation allows estimation of mesophyll conductance in C_4 plants, and reveals that mesophyll conductance decreases as leaves age in both C_4 and C_3 plants. New Phytologist **210**, 875-889.

Bellasio C, Beerling DJ, Griffiths H. 2015. Deriving C_4 photosynthetic parameters from combined gas exchange and chlorophyll fluorescence using an Excel tool: theory and practice. Plant, Cell and Environment doi: 10.1111/pce.12626.

Bellasio C, Burgess SJ, Griffiths H, Hibberd JM. 2014. A high throughput gas exchange screen for determining rates of photorespiration or regulation of C_4 activity. Journal of experimental botany **65**, 3769-3779.

Boyd RA, Gandin A, Cousins AB. 2015. Temperature responses of C_4 photosynthesis: biochemical analysis of Rubisco, phosphoenolpyruvate carboxylase, and carbonic anhydrase in Setaria viridis. Plant Physiology **169**, 1850–1861.

Brown RH, Byrd GT. 1993. Estimation of bundle sheath cell conductance in C_4 species and O_2 insensitivity of photosynthesis. Plant Physiology **103**, 1183-1188.

von Caemmerer S. 2000. Biochemical models of photosynthesis. In Techniques in Plant Sciences p. 196. CSIRO Publishing, Colingwood, Australia.

Von Caemmerer S, Quinn V, Hancock NC, Price GD, Furbank RT, Ludwig M. 2004. Carbonic anhydrase and C_4 photosynthesis: a transgenic analysis. Plant, Cell & Environment **27**, 697-703.

Chi Y, Xu M, Shen R, Yang Q, Huang B, Wan S. 2013. Acclimation of foliar respiration and photosynthesis in response to experimental warming in a temperate steppe in northern China. PLoS One, **8**(2):e56482.

Cousins AB, Baroli I, Badger MR, Ivakov A, Lea PJ, Leegood RC, Von Caemmerer S. 2007. The Role of Phosphoenolpyruvate Carboxylase during C_4 Photosynthetic Isotope Exchange and Stomatal Conductance. Plant Physiology **145**, 1006-1017.

Cousins AB, Ghannoum O, von Caemmerer S, Badger MR. 2010. Simultaneous determination of Rubisco carboxylase and oxygenase kinetic parameters in *Triticum aestivum* and *Zea mays* using membrane inlet mass spectrometry. Plant, Cell and Environment **33**, 444–452.

Dubois JB, Fiscus EL, Booker FL, Flowers MD, Reid CD. 2007. Optimizing the statistical estimation of the parameters of the Farquhar-von Caemmerer-Berry model of photosynthesis. New Phytologist **176**, 402–414.

Ethier GJ, Livingston NJ, Harrison DL, Black TA, Moran JA. 2006 Low stomatal and internal conductance to CO_2 versus Rubisco deactivation as determinants of the photosynthetic decline of ageing evergreen leaves. Plant, Cell and Environment **29**, 2168-2184.

Farquhar GD, von Caemmerer S, Berry JA. 1980 A biochemical model of photosynthetic carbon dioxide assimilation in leaves of 3-carbon pathway species. Planta **149**, 78-90.

Genty B, Briantais J, Baker N. 1989. The relationship between the quantum yield of photosynthetic electron transport and quenching of chlorophyll fluorescence. Biochimica et Biophysica Acta **990**, 87–92.

Gu L, Pallardy SG, Tu K, Law BE, Wullschleger SD. 2010. Reliable estimation of biochemical parameters from C_3 leaf photosynthesis-intercellular carbon dioxide response curves. Plant, Cell and Environment **33**, 1852-1874.

Hatch MD. 1987. C_4 photosynthesis: a unique blend of modified biochemistry, anatomy and ultrastructure. Biochimica et Biophysica Acta **895**, 81-106.

Hatch MD, Burnell JN. 1990. Carbonic anhydrase activity in leaves and its role in the first step of C4 photosynthesis. Plant Physiology **93**, 825–828.

Heckmann D, Schulze S, Denton A, Gowik U, Westhoff P, Weber AP, Lercher MJ. 2013. Predicting C_4 photosynthesis evolution: Modular, individually adaptive steps on a Mount Fuji fitness landscape. Cell **153**, 1579-1588.

Jenkins CLD, Furbank RT, Hatch MD. 1989. Mechanism of C_4 photosynthesis. A model describing the inorganic carbon pool in bundle-sheath cells. Plant Physiology **91**, 1372–1381.

Kromdijk J, Ubierna N, Cousins AB, Griffiths H. 2014. Bundle-sheath leakiness in C_4 photosynthesis: a careful balancing act between CO_2 concentration and assimilation. Journal of experimental botany **65**, 3443-3457.

Miao ZW, Xu M, Lathrop RG, Wang YF. 2009. Comparison of the A-C_c curve fitting methods in determining maximum ribulose 1.5-bisphosphate carboxylase/oxygenase carboxylation rate, potential light saturated electron transport rate and leaf dark respiration. Plant, Cell and Environment **32**, 1191-1204.

Osborne CP, Beerling DJ. 2006. Nature's green revolution: the remarkable evolutionary rise of C-4 plants. Philosophical Transactions of The Royal Society B **361**, 173-194.

Osborne CP, Sack L. 2012. Evolution of C_4 plants: a new hypothesis for an interaction of CO_2 and water relations mediated by plant hydraulics. Philosophical Transactions of The Royal Society B **367**, 583-600.

Pedomo JA, Cavanagh AP, Kubien DS, Galmes J. 2015. Temperature dependence of *in vitro* Rubisco kinetics in species of *Flaveria* with different photosynthetic mechanisms. Photosynthesis Research **124,** 67–75.

Pinto H, Sharwood RE, Tissue DT, Ghannoum O. 2014. Photosynthesis of C_3, C_3–C_4, and C_4 grasses at glacial CO2. Journal of Experimental Botany **65**, 3669-3681.

Sage RF. 2002. Variation in the k_{cat} of Rubisco in C_3 and C_4 plants and some implications for photosynthetic performance at high and low temperature. Journal of Experimental Botany **53**, 609-620.

Savir Y, Noor E, Milo R, Tlusty T. 2010. Cross-species analysis traces adaptation of Rubisco toward optimality in a low-dimensional landscape. Proceedings of the National Academy of Sciences **107**, 3475-3480.

Sharkey TD, Bernacchi CJ, Farquhar GD, Singsaas EL. 2007. Fitting photosynthetic carbon dioxide response curves for C_3 leaves. Plant, Cell and Environment **30**, 1035–1040.

Studer RA, Christin PA, Williams MA, Orengo CA. 2014. Stability-activity tradeoffs constrain the adaptive evolution of Rubisco. Proceedings of the National Academy of Science of the United States of America **111**, 2223–2228.

Ubierna N, Gandin A, Boyd RA, Cousins AB. 2017. Temperature response of mesophyll conductance in three C_4 species calculated with two methods: ^{18}O discrimination and in vitro V_{pmax}. New Phytologist 214, 66-80.

Ubierna N, Sun W, Kramer DM, Cousins AB. 2013. The efficiency of C_4 photosynthesis under low light conditions in *Zea mays*, *Miscanthus* X *giganteus* and *Flaveria bidentis*. Plant, Cell and Environment **36**, 365-381.

Xu LK, Baldocchi DD. 2003 Seasonal trends in photosynthetic parameters and stomatal conductance of blue oak (*Quercus douglasii*) under prolonged summer drought and high temperature. Tree Physiology **23**, 865-877.

Yin X, Struik PC, Romero P, Harbinson J, Evers JB, Van Der Putten PEL, Vos JAN. 2009. Using combined measurements of gas exchange and chlorophyll fluorescence to estimate parameters of a biochemical C_3 photosynthesis model: a critical appraisal and a new integrated approach applied to leaves in a wheat (*Triticum aestivum*) canopy. Plant, Cell and Environment **32**, 448-464.

Yin X, Sun Z, Struik PC, Gu J. 2011a. Evaluating a new method to estimate the rate of leaf respiration in the light by analysis of combined gas exchange and chlorophyll fluorescence measurements. Journal of Experimental Botany **62**, 3489-3499.

Yin XY, Sun ZP, Struik PC, Van der Putten PEL, Van Ieperen W, Harbinson J. 2011b. Using a biochemical C_4 photosynthesis model and combined gas exchange and chlorophyll fluorescence measurements to estimate bundle-sheath conductance of maize leaves differing in age and nitrogen content. Plant, Cell and Environment **34**, 2183-2199.